The structures and vibrations of H_2 monolayers on NaCl, MgO and LiF: similarities and differences

2007 J. Phys.: Condens. Matter 19 305009

(http://iopscience.iop.org/0953-8984/19/30/305009)

IOP PUBLISHING JOURNAL OF PHYSICS: CONDENSED MATTER

J. Phys.: Condens. Matter **19** (2007) 305009 (11pp) doi:10.1088/0953-8984/19/30/305009

The structures and vibrations of H_2 monolayers on NaCl, MgO and LiF: similarities and differences

J Peter Toennies and Franziska Traeger[1]

Max-Planck-Institut für Dynamik und Selbstorganisation, Postfach 2853, Göttingen, Germany

E-mail: traeger@pc.ruhr-uni-bochum.de

Received 5 February 2007, in final form 6 March 2007
Published 13 July 2007
Online at stacks.iop.org/JPhysCM/19/305009

Abstract

A new low-temperature target manipulator ($T_S \simeq 7$ K) has made it possible to extend diffractive and inelastic time-of-flight He atom scattering to the investigation of the structures and external vibrations of the monolayers H_2/NaCl, H_2/MgO and H_2/LiF. On NaCl, H_2 forms a (1×1) monolayer, whereas in the other systems a series of ordered increasingly compressed structures develops with increasing coverage. On MgO these structures are assigned to c(2×2), c(4×2) and c(6×2) phases. On LiF the most stable structure is, in analogy to H_2/MgO, proposed to be close to c(8×2) with a 5% misfit with respect to the LiF substrate. For p-H_2/NaCl, single and overtone vibrational excitations are observed up to the second overtone as well as combinations of a parallel nearly dispersionless mode, at 7.0 meV, and a new dispersive branch with 8.5 meV at the zone boundary. On MgO and LiF three collective vibrations are found. On MgO two non-dispersive perpendicularly polarized modes at 8.5 and 10.5 meV and a dispersive parallel mode at a lower energy are identified. On LiF only one non-dispersive mode at 10.5 meV and two dispersive unassigned modes at lower energies are found. The results for all three systems are compared, and they lead to some general conclusions about dynamical processes on cryogenic films of H_2 on ionic crystals.

1. Introduction

As the simplest of all molecules, H_2 has long served as a benchmark for acquiring a fundamental understanding of molecular structures and dynamics. At the same time the alkali-halide crystal surfaces, because of their ease of preparation by simple cleavage and inherent inertness, have from the beginning of surface physics provided valuable testing grounds. Thus already in the early 1930s, Stern and co-workers were able to carry out their pioneering

[1] Present address: Lehrstuhl für Physikalische Chemie 1, Ruhr-Universität Bochum, 44801 Bochum, Germany.

0953-8984/07/305009+11$30.00

Table 1. Lowest rotational transition energies, intermolecular distances, d, in the bulk and bulk triple point temperatures and pressures for the different H_2 isotopomers and nuclear spin modifications.

	p-H_2	o-H_2	HD	o-D_2	p-D_2
Δj	$0 \rightarrow 2$	$1 \rightarrow 3$	$0 \rightarrow 1$	$0 \rightarrow 2$	$1 \rightarrow 3$
ΔE (meV) [15]	43.93	72.77	11.06	22.20	36.89
d(H_2–H_2) (Å) [16]	3.78	∼3.75	3.70	3.61	3.60
T_{tp} (K)	13.81[a]	—	16.60 [15]	18.69[a]	—
p_{tp} (mbar)	70.22[a]	—	123.7 [15]	170.9[a]	—

[a] Data tables from Leybold Vacuum GmbH, Bonner Str. 498, 50968 Köln, Germany.

experiments on the scattering of molecular beams of H_2 from LiF, NaCl and NaF single-crystal surfaces [1, 2], and these systems are still the subject of current research [3].

A more direct way to study the interaction of H_2 with alkali-halide surfaces is to investigate hydrogen films. Such investigations based on modern surface diagnostic techniques have been hampered by the low temperatures of below 15 K needed to create well-defined films and the inherent insulating nature of adsorbates and substrates. Thus many of the standard surface-science techniques which involve charged particles, such as LEED, EELS and photoelectron spectroscopy (XPS), and also STM, are not easily applied. For this reason most of our knowledge of H_2 films stems from NMR, neutron diffraction and inelastic neutron scattering [4] or infrared spectroscopy [5–7]. The neutron experiments have been limited to a number of substrates such as graphite, boron nitride and MgO, which can be prepared to provide the required large surface areas. Infrared spectroscopy is the only technique which in the past has been successfully applied to H_2 films on alkali halides. The weak dipole moment induced by the substrate surface [5–7] makes it possible to observe the vibrations of the adsorbed H_2 molecules.

As an adsorbate, hydrogen has the advantage of having several isotopomers, H_2, HD and D_2, which differ significantly in their masses. In addition, both H_2 and D_2 have para and ortho nuclear spin modifications. Normal H_2 (n-H_2) consists of 75% odd-j ortho-molecules and only 25 % even-j para-molecules. At the low temperatures of interest, pure para-H_2 (p-H_2) and ortho-D_2 (o-D_2) molecules, which can easily be prepared by conversion on a paramagnetic catalyst surface, are both in the $j = 0$ state. To a good approximation, the $j = 0$ molecules behave as if they were spherically symmetric, whereas the $j = 1$ molecules can be either in the $m = 0$ or in the $m = \pm 1$ state, which are commonly referred to as 'cartwheel' and 'helicopter' orientations, respectively. Thus orientational effects can be isolated by comparing the results for the two nuclear spin modifications. Table 1 lists the lowest rotational transition energies (the vibrational energies are much too high and cannot be excited), the intermolecular distances, d, in the bulk as well as the bulk triple point temperatures and pressures for the different H_2 isotopomers and nuclear spin modifications.

Finally, another rather intriguing reason to study low-temperature H_2 films is the possibility that by virtue of their low masses they may exhibit unusual quantum phenomena such as an extremely large delocalization making them liquid [8] or even possibly superfluid [9].

The present short review summarizes recent studies of H_2 films on MgO, NaCl and LiF made possible by modifying the target manipulator of a helium atom time-of-flight (TOF) scattering apparatus to achieve substrate temperatures down to about 7 K [10, 11]. The results for monolayer and bilayer films of n-H_2, p-H_2, HD and n-D_2 on MgO(001) as well as monolayer films on NaCl(001) were reported previously in [12] and [13], respectively. For both surfaces the structures and external (molecule–surface) vibrational frequencies and dispersion curves

Table 2. Some important properties of the substrates, such as the cation–cation distances, d, in the (001) surface unit cell, the simple cosine corrugation amplitudes for He scattering resulting from an analysis of scattered intensity within the eikonal approximation, ξ, and the physisorption well depth, D, for H_2 and the adsorption energies, E_{ads} for H_2; hel. cat. denotes H_2 in helicopter state adsorbed above a cation; lat. av. stands for laterally averaged potential.

	NaCl	MgO	LiF
d (Å)	3.99 [17]	2.98 [18]	2.84 [19]
ξ (Å)	0.34 [20]	0.15 [21]	∼0.3 [22]
D (meV) (theory)	55 (hel. cat.) [23]	48 (lat. av.) [24]	31 (hel. cat.) [25]
E_{ads} single H_2 (meV) (theory)	35.2 (hel. cat., theory) 28.2 (para cat.) [23]	—	17.3 [24] (lat. av. theory) (lat. av., exp.)
E_{ads} layer (meV) (theory)	42.5 (hel. cat., theory) 34.2 (para) [23]	—	—
E_{ads} layer (meV) (exp.)	38 ± 10 (ortho) 31 ± 10 (para) [5]	28.8 [24]	—
E_{ads} layer (meV) (this work)	40 ± 5 (ortho) 37 ± 5 (para) [13]	22 ± 3 [12]	—

could be measured via diffraction and time-of-flight inelastic scattering during the growth of the films up to completion of a saturated layer. Recently these experiments were extended to n-H_2, p-H_2 and HD films on LiF(001) [14]. Table 2 list some important properties of the three substrates.

2. Collision-induced desorption

In all the previous helium atom scattering (HAS) studies there has been no evidence that the impinging helium atoms had any deleterious effect on the surface as opposed to most other surface probes [26]. This non-destructive feature has in the past always been advertised as one of the unique advantages of HAS. In the course of the present experiments, however, a collision-induced desorption of the H_2 layers by the incident atom beam was observed [14]. The first evidence came from an unexpected behavior of the specular He atom scattering signal during adsorption, a standard method for monitoring film growth. Upon admitting H_2 gas to the target chamber the specular intensity dropped significantly as a result of increased scattering from the isolated adsorbates on the surface and the softness of the nascent H_2 layers. At an incident beam energy of 11 meV this fall-off amounted to more than 95%, which for these scattering conditions was the difference between the reflectivities of the monolayer and the clean surface. Increasing to 40 meV beam energy and beyond, the fall-off decreased and, for example, at 66 meV it became only about 5%. These and other observations were found to be consistent with a collision-induced removal of some of the adsorbed molecules. Thus, in order to maintain an intact layer in the present experiments, He collision energies of less than 40 meV were used. Still, even at these low beam energies, it was necessary to maintain the H_2 pressure at a fixed level to compensate for thermally induced desorption.

3. Experiment

The He beam is produced by expanding 99.9999% pure He gas through a 10 μm nozzle from stagnation pressures which can be adjusted between 10 and 180 bar. By varying the nozzle temperature from 50 to 180 K, nearly monoenergetic ($\frac{\Delta E}{E} \simeq 2\%$) beams with energies between 10 meV ($k_i = 4.4$ Å^{-1}) up to the desorption limiting energy of 40 meV ($k_i = 8.8$ Å^{-1}) are

obtained [11]. A home-made magnetic mass spectrometer, operating in the ion-counting mode, is used to detect the scattered He atoms.

In a fixed-angle geometry ($\theta_i + \theta_f = 90.1°$), diffraction patterns (angular distributions) are measured by rotating the crystal around an axis normal to the plane of the incident and scattered beams. Hence the incident angle θ_i and the final angle θ_f are varied simultaneously. Time-of-flight measurements of the He beam chopped into short pulses allow the detection of energy transfers to and from the atom probe due to the annihilation and creation of surface phonons and/or adsorbate vibrations.

The low-temperature sample holder and cryostat are described in detail in previous publications [13, 12]. The MgO and LiF surfaces were prepared by cleavage in vacuum. For technical reasons, the NaCl surface was cleaved in air and then transferred to the apparatus within a few minutes. The quality of the surfaces was checked by comparison with previous He scattering experiments with the same apparatus. The crystal temperature was measured with an accuracy of about ±1 K with a silicon diode mounted on the sample holder[2,3]. In experiments with the same material the actual temperatures for different sample mountings were calibrated relative to each other by comparing the pressures necessary to maintain an H_2 layer on the surface. In the case of LiF, the loosening of the thermal contacts after several cooling cycles gave an additional absolute uncertainty of ±2 K. Normal-H_2 with a purity of 99.999% from Messer Griesheim[4] was backfilled via a carefully baked gas line through a leak valve into the chamber. The p-H_2 was prepared by conversion of normal-H_2 on an iron oxide and chromium oxide catalyst at ≈20 K in a refrigerator-cooled cryostat. For the experiments on NaCl it was catalytically converted in a dewar of liquid H_2. The p-H_2 content obtained with these methods was previously determined to be considerably greater than 95% [29, 30]. More experimental details can be found in [27, 28].

4. Results and discussion

4.1. Adsorbate sites

Semi-empirical potential calculations [23, 25, 31–33] and infrared spectroscopy of the internal H_2 vibrational frequencies [5–7] provide some insight into the local adsorption sites, not available from the diffraction experiments. For NaCl and LiF it was found that the $j = 0$ and the $j = 1$, $m_j = \pm 1$ 'helicopter' states of the o-H_2 molecules are more strongly bound on cation sites, whereas the $j = 1$, $m_j = 0$ 'cartwheel' states prefer the anion sites [25, 34]. The bonding, however, of the cartwheel states at anion sites under the present conditions with temperatures of 8–11 K is too weak for them to be present. This species could be detected in an infrared experiment by Grunwald and Ewing [7] at a lower temperature of 5.2 K. They interpreted their results in terms of two occupied neighbouring adsorption sites: one above a surface cation, occupied by molecules in $j = 0$, and the other above a surface anion, occupied only by molecules in the $j = 1$ rotational state with 'cartwheel' orientations. The occupation of these close-lying adsorption sites is sterically possible, as the height above an anion site is sufficiently greater than that above an cation because of the different ionic radii. Following arguments by Folman and Kozirovski [35, 36], steric hindrance is also avoided by orienting the molecules at the anion sites perpendicular to the surface with the molecule 3.48 Å above the surface, which is much larger than for the parallel-oriented molecules which lie 2.47 Å above cation sites.

[2] Scientific Instruments Inc., West Palm Beach, FL 33407.
[3] Lake Shore Cryotronics, Inc., 575 McCorkle Blvd, Westerville, OH 43082-8888, USA.
[4] Messer Griesheim GmbH, Fütingsweg 34, 47805 Krefeld, Germany.

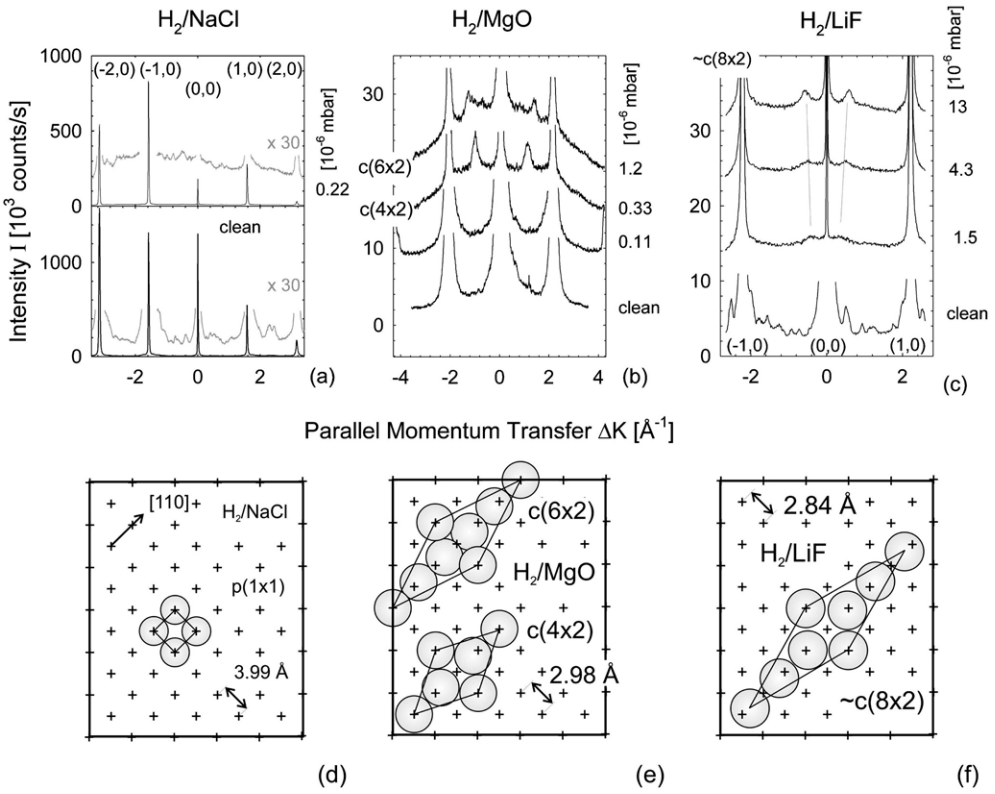

Figure 1. Comparison of the measured angular distributions for n-H_2 films of up to a monolayer on NaCl (a), MgO (b) and LiF (c). The ambient n-H_2 pressures are indicated. The beam energies and surface temperatures were NaCl: $E_i = 22.1$ meV, $T_S = 8$ K; MgO: $E_i = 18.8$ meV, $T_S = 9$ K and LiF: $E_i = 15.2$ meV and $T_S = 11$ K. The corresponding unit cells of the observed structures are shown in (d)–(f) below the angular distributions. The shaded circles represent the area occupied by an H_2 molecule in bulk hydrogen.

4.2. Structures

For clarity, the present discussion will be restricted to H_2 layers, and only data along one crystal direction will be presented. Figure 1 compares the angular distributions along the [110] crystal direction for n-H_2 adsorbates on the three surfaces. In all cases a slight asymmetry in the intensities of the $(+1, 0)$ and $(-1, 0)$ Bragg peaks is visible, which is due to an unavoidable misalignment of the crystal, since the azimuthal angle could not be changed *in situ* in the low-temperature sample holder [13, 12]. The layers were stabilized by maintaining a constant gas pressure of between about 1×10^{-7} and 1.5×10^{-5} mbar in the target chamber.

On NaCl H_2 forms a highly corrugated (1×1) structure with the same periodicity as the substrate. Evidence that indeed an ordered overlayer is formed derives from differences in the relative peak intensities of the specular and first-order diffraction peaks, which are significantly different in comparison with the clean surface. The diffraction intensities remain constant over a wide pressure range following the onset of adsorption up to a maximum pressure of about 10^{-5} mbar, indicating that the monolayer was sufficiently inert to prevent growth of a second layer. The monolayer structure is consistent with semi-empirical potential energy calculations by Briquez *et al* [23]. Only at lower temperatures is a denser structure found, as mentioned above [7].

On NaCl the cation–cation distance, d, is larger than the molecule–molecule distance in bulk H_2, (table 1), but on MgO and LiF d is smaller by 25 and 30%, respectively (table 2). Thus on the latter two surfaces the simplest low-symmetry structure in which the favourable cation adsorption sites are occupied corresponds to a c(2 × 2) arrangement with molecule–molecule distances of 4.02 and 4.21 Å, respectively. A c(2 × 2) structure was seen only on MgO and then only as a transient at low inlet pressures. At higher H_2 gas pressures no peaks were found along the [100] direction, but $\pm 1/2$-order and $\pm 1/3$-order peaks were observed along the [110] direction, respectively; see figure 1(b). These are assigned to the same c(4 × 2) and c(6 × 2) phases seen previously by neutron scattering [37]. A model for a c(4 × 2) phase is given in figure 1(e). This structure and similar c(n × 2) structures with larger unit cells result from a unidirectional compression of rows of hydrogen molecules along the substrate cation rows with the density of the molecules increasing with n. On the NaCl and MgO surfaces the adsorbate structures for the isotopomers H_2, HD and D_2 were found to be the same.

On LiF a transient structure was also seen, but it could not be identified since it was not stable enough for a diffraction analysis. Then, at slightly larger but still low coverage an adsorbate phase develops with a weak additional diffraction peak at a parallel momentum transfer of about $\Delta K = \pm 0.3$ Å^{-1}, which corresponds to about $1/7$ $G_{\pm 1,0}$. Assuming a primitive lattice this indicates a periodicity of about 7 LiF unit cells. Then with further increasing H_2 pressure this peak increases in intensity and shifts outwards to ± 0.58 Å^{-1}, which is close to the $1/4$ $G_{\pm 1,0}$ position. In analogy to the H_2/MgO system a centred structure close to c(8 × 2) symmetry is proposed. Since the exact $1/4$ $G_{\pm 1,0}$ position would be ± 0.55 Å^{-1}, there is a 5% mismatch compared to the exact c(8 × 2) structure. An alternative explanation attributes the diffraction peak to a misfit wavevector between an average space H_2 lattice and the substrate. If a H_2 molecule density of 5 H_2 molecules over 8 Li^+ is assumed, this interpretation leads to the same c(8 × 2) unit cell as proposed above [38, 14].

Finally, it is interesting to notice that on MgO the superstructure diffraction peaks shift as expected for the transformation of small adsorbate unit cells into larger cells, similar to Oswald ripening. In the case of H_2/LiF, the shift would seem to suggest an opposite trend, even though the coverage increases towards the c(8 × 2) phase as concluded from the applied H_2 gas pressures. A possible explanation would be the formation of a primitive structure first, in which all peaks are visible, followed by a centred structure at larger coverages, in which every second peak vanishes due to the centred symmetry. However, this explanation does not account for a continuous peak shift.

4.3. Adsorbate vibrations

Figure 2 compares some selected TOF spectra, which show most clearly the features characteristic for each particular system. They were recorded at somewhat different incident angles and slightly different incident energies. For this reason they are normalized to the diffuse elastic peak, which, of course, depends on the defect density, information which is lost by this procedure. Since the adsorbate vibrational frequencies depend on the mass as expected for a harmonic oscillator, only the results for H_2 are discussed here.

Figure 3 summarizes the dispersion curves in irreducible zone schemes for the three systems. The largest inelastic signal is observed in the case of H_2/NaCl, which also shows as many as nine inelastic peaks, more than for the other surfaces. The sharpness of some of the peaks and the relatively low diffuse elastic peak intensities and sharp diffraction peaks all confirm the excellent ordering of the H_2 layer. Largely based on the calculations of Briquez [23] and other observations [13], all the distinct peaks are assigned to the fundamental frequency and all overtones up to the second of the frustrated translational vibrations (T-mode). The

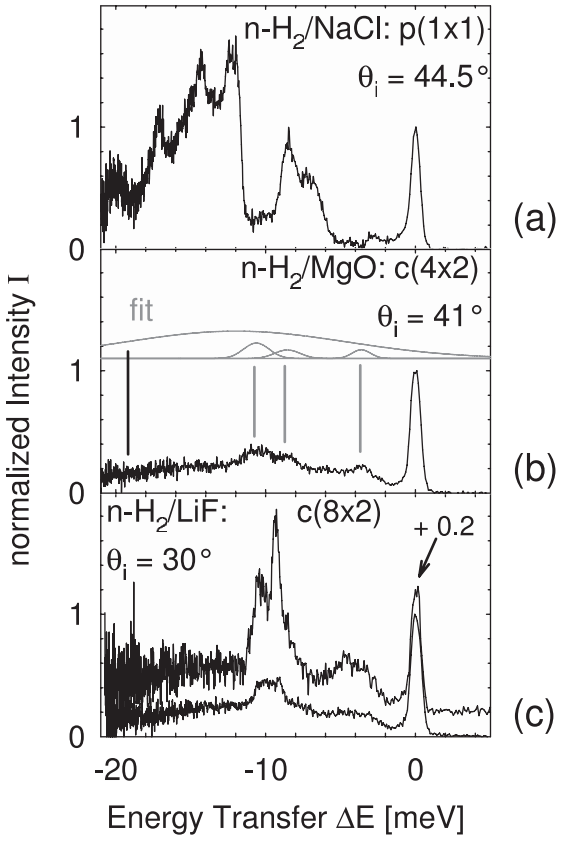

Figure 2. Comparison between TOF spectra of monolayers of n-H_2 on (a) NaCl, (b) MgO, and (c) LiF measured along the [110] crystal direction. The experimental conditions were (a) $\theta_i = 44.5°$, $E_i = 26.5$ meV, $T_S = 8$ K, $P(n\text{-}H_2) = 9 \times 10^{-8}$ mbar; (b) $\theta_i = 41.0°$, $E_i = 28.8$ meV, $T_S = 9$ K, $P(n\text{-}H_2) = 3.3 \times 10^{-7}$ mbar and (c) $\theta_i = 30.0°$, $E_i = 26.6$ and 26.8 meV, $T_S = 11$ K, $P(n\text{-}H_2) = 1.7 \times 10^{-6}$ mbar (upper spectrum) and $P(n\text{-}H_2) = 6.5 \times 10^{-6}$ mbar (lower spectrum).

0.7–1.0 meV differences in the spectra measured with n-H_2 and p-H_2 indicate that the p-H_2 T-mode frequencies are about 10% smaller than for o-H_2. In the case of HD, one mode at $\Delta E = 7.6$ meV could possibly be due to excitation of 2D rotations of the adsorbed molecule. This is the only case in which an internal degree of freedom may have been involved.

In the monolayer n-H_2/MgO, the diffuse elastic peak is much larger and the single-phonon peaks are superimposed on a relatively intense inelastic background. The TOF spectra reveal altogether only three modes, two Einstein modes at 9 and 11 meV which do not depend on the wavevector Q, and a dispersive mode at lower frequencies with a maximum frequency of about 7 meV. The Einstein modes are assigned to collective modes with vertical polarization and the dispersive mode is thought to be due to a T-mode directed along the short axis of the c(4 × 2) unit cell. In view of the inherently broad inelastic peaks the differences between the ortho and para frequencies are largely smeared out. From measurements along [100] the frequencies for p-H_2 are estimated to be smaller than for o-H_2 by about 0.9 meV. The width of the peak indicated that also in this case—and also for HD—two modes are present.

MgO was the only surface for which a second layer with a (1 × 1) structure could be formed at higher dosages. With two layers only a non-dispersive mode was observed at 5 meV.

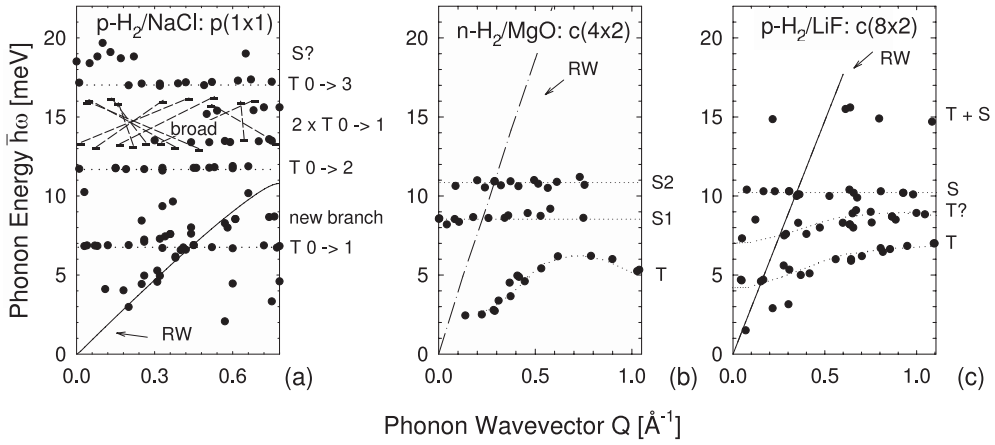

Figure 3. Dispersion curves of the external vibrations of a monolayer of p-H_2/NaCl(001) (a), n-H_2/MgO (b) and p-H_2/LiF (c) along the [110] crystal direction. The H_2 gas pressures were 1×10^{-7}, 3.3×10^{-7} and 2×10^{-6} mbar, and the crystal temperatures 8, 9 and 11 K, respectively. The dotted lines are guides to the eye.

For the c(8×2) layer of p-H_2 on LiF three modes are clearly seen. A dispersionless mode at 10.5 meV is assigned to a perpendicularly polarized S-mode similar to the two modes at about 10 meV found on MgO. In addition, two weakly dispersive modes are found with maximum energies of 7 and 9 meV at the zone boundary. At least one of these appears to be due to a T-mode polarized parallel to the surface. The n-H_2/LiF spectra are less structured and broadened compared to p-H_2. A non-dispersive mode at about 10 meV similar to the one with p-H_2 could be clearly identified. Only one additional dispersive mode which, however, could be followed up to the zone boundary, where it had an energy of 10 meV, was seen. To what extent these differences are due to the o-H_2 component is not understood. The assignment is complicated by the possibility that the relative ortho to para concentrations may be much different on the surface than in the equilibrium gas. For example, on NaCl p-H_2 was found to be significantly enriched [6, 13].

It is also interesting to compare a good-quality and a poor-quality spectrum of H_2/LiF with the spectrum of the adsorbate on MgO. The poor-quality spectrum of H_2/LiF was obtained from an adsorbate which had a considerable amount of impurities. Although the crystal was heated and the H_2 monolayer was readsorbed after each one or two TOF spectra, at the end of long experiments contaminations, e.g. CO, had accumulated in the chamber. During the TOF measurements these more strongly bound molecules were partially displacing the H_2 and could later be detected by a second desorption step in thermal desorption curves. Under these conditions the TOF spectra were of poorer quality, as indicated by large intensities of the diffuse elastic peak relative to the inelastic peaks; compare the TOF spectra in figure 2(c). In further experiments it was proven that different H_2 pressures did not account for the changes. This sensitivity of the TOF signal to contaminations acting as defects together with the strong similarity of the spectrum to that for H_2/MgO would seem to suggest that the MgO surface was also contaminated. This would be in variance with an interpretation which explains the broader lower-intensity signals on MgO as a result of lower corrugation and a lower contribution of lateral forces acting on the adsorbed H_2 molecule. However, a significant contamination could be ruled out by the absence of the expected features in thermal desorption spectroscopy (TDS) desorption curves. Still it is a possibility that defects were inherent to the H_2 films or induced

Table 3. Comparison of the major results from the three systems.

	H_2/NaCl	H_2/MgO	H_2/LiF
Structures	$p(1 \times 1)$ commensurate	$c(2 \times 2) \rightarrow$ $c(4 \times 2) \rightarrow$ $c(6 \times 2)$	Transition phase $\rightarrow$ incommensurate $\sim c(8 \times 2)$
Corrugation of the overlayer	Greater than substrate	Same as for substrate	?
Vibrations	Non-dispersive T-modes $\hbar\omega = 7.0$ meV $(0 \rightarrow 1)$ $= 11.8$ meV $(0 \rightarrow 2)$ $= 17.2$ meV $(0 \rightarrow 3)$	$c(4 \times 2)$ and similarly $c(6 \times 2)$ non-dispersive S-modes $\hbar\omega = 8.5$ meV $(0 \rightarrow 1)$ $= 10.5$ meV $(0 \rightarrow 1)$ dispersive T-mode $\hbar\omega \simeq 6$ meV	Non-dispersive S-mode $\hbar\omega = 10.5$ meV Two dispersive modes $\hbar\omega \simeq 7$ meV $\hbar\omega \simeq 9$ meV
Multiphonons	Only overtones	Intensive diffuse background	Small diffuse background
Comments	—	Second layer seen	—

by the defects of the MgO substrate. This is also in accord with the rather broad half-order diffraction peaks in the angular distribution; see figure 1(b).

5. Summary

These experiments represent the first extensive studies of the structures and vibrations of H_2 monolayers on NaCl, LiF and MgO. Table 3 provides an overview of the results of our experiments. While for H_2/NaCl a robust (1×1) structure is found, in H_2/MgO and H_2/LiF the cation site–site spacings are too small for a hypothetical (1×1) structure and too large for a simple $c(2 \times 2)$ arrangement. In order to accommodate the H_2–H_2 attractions, increasingly dense centred structures are observed, which are proposed to originate from compression of a $c(2 \times 2)$ structure. Most stable are the $c(4 \times 2)$ and $c(6 \times 2)$ structures for the MgO substrate and $c(8 \times 2)$ for the LiF substrate. Thus these latter more complicated structures result from a competition between the H_2–cation attraction and the H_2–H_2 repulsion. A more detailed structure for H_2/LiF will be proposed in a forthcoming article [14]. And indeed there is some evidence from molecular dynamics calculations [32, 33] that the structures on MgO and LiF may not be as simple as in the models of figure 1.

The cation lattice spacing also has a dominant effect on the adsorbate lattice vibrations. Thus, the predominance of dispersionless T-mode excitations on NaCl is also easily explained in terms of the large spacing of the H_2 molecules, which allows the molecules to vibrate parallel to the surface without disturbing each other. The lack of strong evidence for a vertical polarized S-mode on NaCl probably can be explained by its energy being too high to be excited. In semi-empirical potential calculations its frequency is estimated to be about 18.1 meV; thus the occasionally observed small peaks at around 19 meV might be assigned to S-mode excitations [13].

The more complicated dispersion curves found for the MgO and LiF surfaces, some with significant dispersion, result from the strong coupling between the H_2 molecules, and a full understanding will require a careful detailed molecular dynamics analysis. For example, for CO_2/NaCl [39] altogether 20 distinct modes were predicted of which the dispersion curves of eight with maximum energies below 9.5 meV could be detected [40]. A similar analysis for the systems studied here will be more challenging because of the necessity to include quantum effects.

The results obtained so far would seem to suggest that these substrates are not prime candidates for achieving superfluid layers [8, 9]. Of course much lower temperatures of the order of less than 2.4 K would be required to test for a superfluid transition [13]. At the much higher temperatures of the present study, however, these systems appear to behave as if they were classical systems. On NaCl the high vibrational frequencies and several overtones combined with the sharp diffraction peaks suggest that the molecules are tightly bound at cation sites. The large multiphonon background and broad diffraction peaks, which—we feel most likely—are due to either disorder of the substrate or of the adlayers, might, of course, alternatively be a result of quantum delocalization. On LiF, on the other hand, the substrate is considered to be especially ideal so that defects are less likely, giving more room for quantum delocalization as a possible explanation for the broad inelastic intensity and large diffuse elastic peak.

Acknowledgments

The authors would like to thank Professor L W Bruch and Professor D B Jack for very helpful discussions.

References

[1] Estermann I and Stern O 1930 *Z. Phys.* **61** 95
[2] Frisch R 1933 *Z. Phys.* **84** 443
[3] Ekinci Y and Toennies J P 2005 *Phys. Rev.* B **7220** 205430
[4] Wiechert H 2003 *Adsorbed Layers on Surfaces* (*Landolt-Börnstein* Group III *Condensed Matter* volume A1/2001) (Berlin: Springer)
[5] Heidberg J, Voßberg A, Hustedt M, Thomas M, Briquez S, Picaud S and Girardet C 1999 *J. Chem. Phys.* **110** 2566
[6] Briquez S, Picaud S, Girardet C, Hoang P N M, Heidberg J and Voßberg A 1998 *J. Chem. Phys.* **109** 6435
[7] Grunwald M and Ewing G E 1998 *J. Chem. Phys.* **109** 4990
[8] Vilches O E 1992 *J. Low Temp. Phys.* **89** 267
[9] Gordillo M C and Ceperley D M 1997 *Phys. Rev. Lett.* **79** 3010
[10] Schmicker D 1991 *PhD Thesis* Universität Göttingen, Bericht Max-Planck-Institut für Strömungsforschung
[11] Traeger F 2001 *PhD Thesis* Universität Göttingen, Bericht Max-Planck-Institut für Strömungsforschung
[12] Skofronick J G, Toennies J P, Traeger F and Weiss H 2003 *Phys. Rev.* B **67** 035413
[13] Traeger F and Toennies J P 2004 *J. Phys. Chem.* B **108** 14710
[14] Toennies J P and Traeger F 2007 in preparation
[15] Souers P C 1986 *Hydrogen Properties for Fusion Energy* (Berkeley, CA: University of California Press)
[16] Manzhelii V G and Freiman Y A (ed) 1997 *Physics of Cryocrystals* (New York: AIP) Tab. 4.2
[17] *Gmelins Handbuch der Anorganischen Chemie, System-Nr. 21* in *Natrium* 1973 **8** suppl. 6 (Weinheim: Verlag Chemie)
[18] *Magnetic Oxides and Related Compounds* (*Landold-Börnstein* vol V) (Berlin: Springer)
[19] Brusdeylins G, Bruce Doak R and Toennies J P 1983 *Phys. Rev.* B **44** 3662
[20] Glebov A L 1997 *PhD Thesis* Universität Göttingen, Bericht Max-Planck-Institut für Strömungsforschung
[21] Benedek G, Brusdeylins G, Senz V, Skofronick J G, Toennies J P, Traeger F and Vollmer R 2001 *Phys. Rev.* B **64** 125421
[22] Boato G, Cantini P and Mattera L 1976 *Surf. Sci.* **55** 141
[23] Briquez S 1997 *PhD Thesis* Université de Franche-Comté, Besançon, France
[24] Vidali G, Ihm G, Kim H-Y and Cole M 1991 *Surf. Sci. Rep.* **12** 133
[25] Kroes G-J and Mowrey R C 1995 *J. Chem. Phys.* **103** 2186
[26] Toennies J P, Traeger F, Vogt J and Weiss H 2004 *J. Chem. Phys.* **120** 11347
[27] Toennies J P and Vollmer R 1991 *Phys. Rev.* B **44** 9833
[28] Toennies J P 1991 *Surface Phonons* (*Springer Series in Surface Science* vol 21) ed W Kress and deWette (Berlin: Springer)
[29] Tappe U 1996 private communication

[30] Josefowski L, Ottinger Ch and Rox T 1992 *Chem. Phys. Lett.* **190** 323
[31] Kroes G-J and Mowrey R C 1995 *Chem. Phys. Lett.* **232** 258
[32] Jack D B 2006 private communication
[33] Sallabi A and Jack D B 2007 *Surf. Sci.* at press
[34] Bertino M F, Glebov A L, Toennies J P, Traeger F, Pijper E, Kroes G J and Mowrey R C 1998 *Phys. Rev. Lett.* **81** 5608
[35] Day D J and Ewing G E 1994 *J. Chem. Phys.* **100** 8432
[36] Folman M and Kozirovski Y 1972 *J. Colloid Interface Sci.* **38** 51
[37] Degenhardt D, Lauter H J and Haensel R 1987 *Proc. 18th Conf. on Low Temperature Physics (Kyoto, 1987)*; *Japan. J. Appl. Phys.* **26** 341
[38] Bruch L W 2003 private communication
[39] Picaud S, Hoang P N M and Girardet C 1995 *Surf. Sci.* **322** 381
[40] Lange G, Schmicker D, Toennies J P, Vollmer R and Weiss H 1995 *J. Chem. Phys.* **103** 2308